Molecular Reorientation of Liquid Water studied with Femtosecond Mid-infrared Spectroscopy

H. J. Bakker, Y. L. A. Rezus and R. L. A. Timmer

FOM Institute AMOLF, Kruislaan 407, 1098 SJ Amsterdam, The Netherlands

(February 13, 2008)

Abstract

The molecular reorientation of liquid water is key to the hydration and stabilization of molecules and ions in aqueous solution. A powerful technique to study this reorientation is by measuring the time-dependent anisotropy of the excitation of the O–H/O–D stretch vibration of HDO dissolved in D_2O/H_2O using femtosecond mid-infrared laser pulses. In this paper we present and discuss experiments in which this technique is used to study the correlation between the molecular reorientation of the water molecules and the strength of the hydrogen-bond interactions. It is found that a sub-ensemble of the molecules that have weak donated hydrogen bonds shows a surprisingly fast ($\sim$100 fs) reorientation that is accompanied by a large change of the vibrational frequency. This sub-ensemble absorbs in the blue wing of the hydroxyl absorption band, and is constantly replenished as a result of the collective hydrogen-bond dynamics of liquid water that shows an average time constant of $\sim$700 fs. The combination of the reorientation in the blue wing and the hydrogen-bond dynamics leads to an effective molecular reorientation time of liquid water of 2.5 ps. This mechanism largely agrees with the molecular jumping mechanism for the reorientation of liquid water that has recently been proposed by Laage and Hynes [1,2].

INTRODUCTION

Many of the characteristic properties of liquid water find their origin in the large number of directional hydrogen-bond interactions present in this liquid. In spite of the strength and high concentration of these hydrogen-bond interactions, water molecules turn out to be surprisingly mobile. As a result, liquid water is extremely fast in rearranging its molecules to enable the solvation of reactants and to take up dissipated energy [3–6]. An important aspect of this rearrangement is the molecular reorientation of the water molecules.

The molecular reorientation of liquid water has been studied with several experimental techniques like NMR [7–9], dielectric relaxation [10,11], and THz absorption spectroscopy [12,13]. With these techniques consistent results concerning the rate of molecular reorientation in liquid water were obtained. However, an unfortunate characteristic of these techniques is that only the average reorientation can be measured, and that it is not possible to probe the orientational dynamics of sub-ensembles of the water molecules.

The molecules in liquid water show a large variation in hydrogen-bond configurations and associated hydrogen-bond lengths and angles [14–17]. As a result, the absorption bands of the O–H/O–D stretch vibrations of water molecules (that absorb at 3/4 μm) are strongly inhomogeneously broadened: water molecules with long and bent hydrogen bonds absorb at higher frequencies than water molecules with short and linear hydrogen bonds. With femtosecond mid-infrared spectroscopy it is possible to spectrally select a sub-ensemble of water molecules and to measure its specific dynamics, like for instance the fluctuations of the hydrogen-bond network [18–27] or the molecular reorientation [28–35].

The measurement of the orientational dynamics of water via the excitation of the O–H/O–D stretch vibrations relies on the fact that the rotation of the molecule changes the direction of the vibrational transition dipole moment. This method does not work if there are other processes contributing to the change of the direction of the transition dipole moment, like intramolecular and/or intermolecular resonant (Förster) energy transfer between the vibrations. As a result, it is unfortunately not possible to measure the

orientational dynamics of the molecules in pure liquid H_2O [3]. Consequently, the reported femtosecond mid-infrared measurements of the orientational dynamics of water always refer to HDO molecules dissolved in either normal or heavy water. In both cases the dynamics of a hydroxyl group (either O–H or O–D) embedded in a network of isotopically distinct hydroxyl groups are studied. Studying the orientational dynamics of the O–H stretch vibration of HDO:D_2O has the advantage that it is easier to resolve dynamical inhomogeneities, as the O–H stretch vibration of HDO:D_2O is more strongly inhomogeneously broadened than the O–D vibration of HDO:H_2O [22,25]. On the other hand, studying the O–D vibration of HDO:H_2O has the advantage that the lifetime of the O–D vibration is more than two times longer than that of the O–H vibration, thereby allowing the measurement of the orientational dynamics of the O–D group over a significantly longer time interval.

In this Feature Article we will review the studies of the orientational dynamics of liquid water with femtosecond mid-infrared spectroscopy of HDO:D_2O [28–32] and HDO:H_2O [33–35]. We will describe the experiments, the methods by which information on the orientational dynamics has been extracted from the data, and the interpretation of the data in terms of molecular orientational mobilities. We also compare the experimental findings with the results of molecular dynamics simulations of the reorientation of liquid water [1,2,15] that in part were inspired by the experimental studies. We also include recent experimental results that resolve some apparent inconsistencies between previous experimental findings for the O–H and the O–D vibrations.

EXPERIMENTAL

The orientational dynamics of the O–H/O–D stretch vibrations of HDO dissolved in D_2O/H_2O have been studied with polarization-resolved pump-probe spectroscopy [28–35]. In all experiments, the femtosecond mid-infrared pump and probe pulses are generated via a sequence of nonlinear frequency-conversion processes that are pumped by the output of a Ti:sapphire multi-pass and/or regenerative amplifier (800 nm, 1 kHz, pulse energy $\geq$1 mJ).

The mid-infrared pump have a wavelength of ∼3 μm (=∼ 3300 cm^{-1}) or ∼4 μm (=∼ 2500 cm^{-1}), depending on whether the O–H or the O–D stretch vibration is being studied.

Pump and probe pulse generation

In most studies the pump pulses are generated via an optical parametric amplification process in a KTP or $KNbO_3$ crystal that is pumped by a part of the 800 nm pulses of the Ti:sapphire laser. To generate 3 or 4 μm pulses in the parametric amplification, the process has to be seeded by 1100 or 1000 nm light, respectively. This seed has been produced with different methods. In one method, a fraction of the 800 nm light is used to generate a white-light continuum [31,32]. Part of this continuum at 1100/1000 nm is parametrically amplified in a BBO (β-bariumborate) crystal. This process is pumped either by the second harmonic at 400 nm of part of the 800 nm pulse [31], or by part of the fundamental 800 nm pulse [32]. The resulting light pulses at 1100/1000 nm are sufficiently strong to seed the parametric amplification process in KTP [31] or $KNbO_3$ [32]. An alternative method to generate the seed pulses is by parametric generation or white-light generation followed by parametric amplification in BBO to generate pulses with wavelengths of 1300-1400 nm (signal) and 2000-2200 nm (idler) [29,30,34,35]. Subsequently, the idler pulses are frequency doubled to pulses with a wavelength of 1000-1100 nm in a second BBO crystal, and these pulses then serve as seed in a parametric amplification process in KTP [29,30,35] or $KNbO_3$ [34]. In the experiment of Ref. [33], the pump pulses at 4 μm are generated via difference frequency mixing of pulses with wavelengths of ∼1330 nm and ∼2000 nm in a $AgGaS_2$ crystal. These latter pulses are generated via white-light seeded optical parametric amplification in BBO (Spectraphysics OPA) that is pumped by a fraction of the 800 nm pulses.

The energy of the generated pump pulses varies between 2 μJ [33] and 10 μJ [28–31,34,35]. In some studies, the used KTP and $KNbO_3$ crystals are quite short (1 mm) and the 800 nm pulses have a pulse duration of 30 [32] or 40 fs [33]. The resulting mid-infrared pulses are ultrashort, having a pulse duration of ∼50 fs [32,33]. The bandwidth of these puleses

is ∼400 cm^{-1}, thus covering completely the O–H/O–D absorption band. In other studies, longer crystals (4-5 mm) and longer 800 nm pulses (∼ 100 fs) have been used, leading to the generation of substantially longer (∼150 fs) mid-infrared pump pulses with a much narrower spectral bandwidth of ∼100 cm^{-1} [28–31,34]. In Fig. 1 various pump spectra are presented that are resonant with different parts of the O–H stretch absorption band of HDO:D_2O.

The probe pulses have also been generated with a variety of methods. In some of the experiments [28,32–35] the probe pulses are obtained by splitting off a small fraction of the pump pulse. In other experiments, independently tunable probe pulses are generated by a separate sequence of nonlinear frequency-conversion processes [29–31]. This sequence can be the same as that used to generate the pump pules [31]. In Refs. [29,30] the probe pulses were generated with the same sequence of frequency conversion processes that was used to generate the pump and probe pulses in Ref. [33], i.e. difference frequency mixing in $AgGa_2$ of the signal (1300-1400 nm) and idler (2000-2200 nm) pulses that are generated via white-light seeded optical parametric amplification in BBO.

Vibrational saturation spectroscopy

The pump and probe pulses are focussed to the same spot in the sample. In case the O–H stretch vibration is studied, the solvent is D_2O, and the concentration of HDO is ∼1%. In case the O–D stretch vibration is studied, the solvent is H_2O, and the concentration of HDO is 4%. In the latter experiments a higher concentration has to be used, because the H_2O solvent has a non-negligible absorption in the frequency region of the O–D stretch vibration. Nevertheless, the concentration of O–D oscillators is still sufficiently low to avoid effects of resonant vibrational Förster energy transfer among the O–D vibrations. The samples are either contained in a sample cell with CaF_2 windows [28–31,33,34] or flowed as a 50 μm path length jet [32]. The pump excites a few percent of the O–D/O–H stretch vibration of the HDO molecule from the $v = 0$ ground state to the $v = 1$ excited state. This excitation leads to a bleaching effect at the fundamental transition frequencies due

to a decrease of the $v = 0 \rightarrow 1$ absorption and the presence of $v = 1 \rightarrow 0$ stimulated emission. The excitation also leads to induced absorption at frequencies corresponding to the $v = 1 \rightarrow 2$ transition. The latter absorption is redshifted with respect to the fundamental transition by 270/200 cm^{-1} due to the anharmonicity of the O–H/O–D stretch vibration. In some experiments, the transmitted probe light is measured spectrally integrated by a PbSe [28–31] or an InSb [32] detector, in others the transmitted probe is dispersed with a monochromator and detected spectrally resolved by the 32 elements of a MCT (mercury-cadmium-telluride) detector array [33–35]. In all experiments, a small fraction of the probe is split off and used as a reference to correct for the shot-to-shot probe pulse energy fluctuations. In most experiments this reference is measured spectrally integrated [28,29,31–33], but in some experiments the reference is spectrally dispersed in the same way as the probe and detected by another 32 element MCT detector array, thus allowing for a frequency-resolved correction for shot-to-shot fluctuations in the probe-pulse energy [34,35].

Anisotropy of the excitation

The rate of molecular reorientation of the water molecules is studied by measuring the time dependence of the anisotropy of the excitation of the O–H/O–D stretch vibration. In most experiments, the polarization of the pump is rotated before the sample at 45° with respect to the probe polarization with a $\lambda/2$ plate. After the sample, the polarization components of the probe parallel and perpendicularly to the pump polarization are alternatingly chosen using a polarizer [28,29,31,32,34,35]. In Ref. [33], the experiment is performed with a probe pulse that has a polarization that is parallel to the pump polarization, and a probe pulse with a polarization at the magic angle (54.7 °) with respect to that of the pump.

The signals measured are the ratios of the transmitted probe and reference beams: $T_{\parallel} = I_{\parallel}/I_{\mathrm{ref}}$, $T_{\perp} = I_{\perp}/I_{\mathrm{ref}}$, and $T_{\mathrm{iso}} = I_{\mathrm{iso}}/I_{\mathrm{ref}}$, where I_{iso} represents the signal measured by a probe pulse with its polarization at the magic angle. To determine the pump-induced changes $T_{\parallel}$, $T_{\perp}$ and T_{iso}, the signals are alternatingly measured with and without the pump

pulse present using a 500 Hz chopper in the pump beam. The signals are used to construct the absorption changes $\Delta\alpha_{\parallel} = \ln[T_{\parallel}/T_0]$, $\Delta\alpha_{\perp} = \ln[T_{\perp}/T_0]$, and $\Delta\alpha_{\rm iso} = \ln[T_{\rm iso}/T_0]$ where T_0 represents the transmission signal in the absence of the pump. From $\Delta\alpha_{\parallel}$ and $\Delta\alpha_{\perp}$, the rotational anisotropy [36] can be constructed:

$$R = \frac{\Delta\alpha_{\parallel} - \Delta\alpha_{\perp}}{\Delta\alpha_{\parallel} + 2\Delta\alpha_{\perp}} = \frac{\Delta\alpha_{\parallel} - \Delta\alpha_{\perp}}{3\Delta\alpha_{\rm iso}}. \tag{1}$$

The anisotropy can also be obtained from $\Delta\alpha_{\parallel}$ and $\Delta\alpha_{\rm iso}$ [33]:

$$R = \frac{\Delta\alpha_{\parallel} - \Delta\alpha_{\rm iso}}{2\Delta\alpha_{\rm iso}}. \tag{2}$$

The denominator of equations (1) and (2) is not affected by the reorientation [36]. Hence, isotropic effects like vibrational relaxation and spectral diffusion are divided out.

VIBRATIONAL RELAXATION

Experimental results

In Fig. 2, transient absorption spectra are shown at different delays after exciting the O–H stretch vibration of HDO:D_2O with a pump pulse centered at 3400 cm^{-1} (upper panel) and the O–D stretch vibration of HDO:H_2O with a pump pulse centered at 2500 cm^{-1} (lower panel). At early delays, the transient spectra show the pump-induced bleaching of the fundamental $v = 0 \rightarrow 1$ transition for probe frequencies >3250/2425 cm^{-1} and the induced $v = 1 \rightarrow 2$ absorption at probe frequencies <3250/2425 cm^{-1}. At longer delays (>3 ps) transmission changes are observed that persist over the experimentally accessible time range (500 ps) and that have the character of a bleach on the red side of the spectrum and of an induced absorption on the blue side. These persistent transient spectra reflect the temperature rise in the sample that results from the absorption and thermalization of the energy of the pump pulse. A rise in temperature induces a blue shift and a decrease in cross section of the O–H/O–D vibrations [33–35].

In Fig. 3 the isotropic absorption changes are shown as a function of delay between pump and probe for three different probe frequencies. At probe frequencies of 3400/2500 cm^{-1} the signal is dominated by a decaying bleach, whereas at 3170/2390 cm^{-1} the signal consists of a decaying induced absorption. In between these two frequencies more complicated dynamics are observed, especially for the O–D vibration. For a probe frequency of 2435 cm^{-1}, a bleaching signal is observed that shows a decay followed by a re-rise to a constant (bleached) end level. The latter ingrowing part of the signal reflects the temperature increase of the sample in the focus of the pump beam. The fact that the signal turns over shows that the temperature rise takes place on a slower timescale than the relaxation of the O–D stretch vibration, which implies that the vibrational relaxation proceeds via a non-thermal intermediate state.

The signal at large delays, that represents the effect of the increase in temperature, is isotropic, meaning that the magnitude of this signal is the same for $\Delta\alpha_{\parallel}$ and $\Delta\alpha_{\perp}$. Hence, to obtain the anisotropy of the excited O–H/O–D vibration, the time-dependent thermalization signal has to be subtracted from $\Delta\alpha_{\parallel}$ and $\Delta\alpha_{\perp}$. To determine the delay dependence of the thermalization signal, the spectral responses of the O–H and the O–D vibration are fitted to a relaxation model that was developed in Refs. [33,34,37]. This model is described in Appendix A and illustrated in Fig. 4. In this model the relaxation model proceeds via relaxation with time constant $\tau_1 = 1/k_1$ to an intermediate state. This latter state relaxes with time constant $\tau_* = 1/k_*$ to the final state in which the energy has become thermal. The two time constants τ_1 and τ_* are treated as global fit parameters, and the cross-sections of the transitions between the vibrational levels are allowed to vary over the spectrum. The resulting fits are represented by the solid lines in Figs. 2 and 3. It is seen that the model provides an accurate description of the data, which implies that spectral diffusion effects do not play an important role after a delay of 0.4 ps for pump pulses that are resonant with the center of the absorption bands. For the O–H stretch vibration of HDO dissolved in D_2O τ_1=0.7±0.1 ps and τ_*=0.6±0.1 ps. For the O–D stretch vibration of HDO dissolved in H_2O τ_1= 1.8±0.2 ps and τ_*=0.9±0.1 ps.

ORIENTATIONAL DYNAMICS

Extracting the anisotropy of the vibrational excitation

To infer the anisotropy of the excitation from the data, the spectral component corresponding to the heating effect (as obtained from the isotropic spectral dynamics) is subtracted from both $\Delta\alpha_{\parallel}$ and $\Delta\alpha_{\perp}$. Figure 5 shows the resulting $\Delta\alpha_{\parallel}$ and $\Delta\alpha_{\perp}$ for the O–H stretch vibration of HDO:D_2O and the O–D stretch vibration of HDO:H_2O. There is a striking difference between the two vibrations. For the O–D stretch vibration, $\Delta\alpha_{\parallel}$, $\Delta\alpha_{\perp}$ and $\Delta\alpha_{\mathrm{iso}}$ decay more or less simultaneously. In contrast, for the O–H stretch vibration, $\Delta\alpha_{\parallel}$ and $\Delta\alpha_{\perp}$ are observed to show still significant amplitudes that are opposite in sign after $\Delta\alpha_{\mathrm{iso}}$ has become nearly equal to zero. The anisotropy calculated from the curves in the upper panel of Fig. 5 is shown in Fig. 6a. The obtained anisotropy diverges to infinity, from which it is clear that this curve cannot represent the orientational dynamics of the O–H stretch vibration.

The sign of the residual signals of $\Delta\alpha_{\parallel}$ and $\Delta\alpha_{\perp}$ does not depend on whether the original signal is a bleach or an induced absorption [35]. At all frequencies, $\Delta\alpha_{\parallel}$ shows a residual bleaching while $\Delta\alpha_{\perp}$ shows a residual absorption. Figure 6b shows that the amplitude of the residual signal closely follows the linear absorption spectrum of the O–H stretch vibration. The presence of these residual signals, i.e. non-zero $\Delta\alpha_{\parallel}$ and $\Delta\alpha_{\perp}$ at delays at which there are no excited molecules left ($\Delta\alpha_{\mathrm{iso}} = 0$), implies that the vibrational relaxation of the O–H stretch vibration results in a distribution of ground state molecules that is anisotropic: after relaxation there are more OH groups aligned perpendicular to the pump than there are aligned parallel to it.

The observation of an anisotropic ground state following vibrational relaxation likely follows from a difference in orientational mobility of excited and non-excited O–H groups. Directly after the excitation, excited O–H oscillators are oriented preferentially along the pump polarization while the non-excited O–H oscillators are oriented preferentially perpen-

dicular to the pump polarization. In case the excited and the non-excited oscillators would show the same orientational dynamics, the relaxation of the excited oscillators would restore an isotropic distribution of ground state O–H oscillators, because the anisotropy of the relaxed oscillators cancels exactly the (opposite) anisotropy of the non-excited oscillators. However, if the excited oscillators show a faster or slower orientational relaxation at some stage during their relaxation, the distribution of the ground state O–H oscillators following relaxation will be anisotropic. The eventual depletion of ground-state O–H oscillators that are polarized along the pump polarization indicates that the excited oscillators show a larger orientational mobility at some stage during the relaxation than the non-excited oscillators. Due to this higher orientational mobility, the relaxed O–H oscillators will be more isotropic than the non-excited oscillators. The sum of the relaxed oscillators and the non-excited oscillators will add up to a distribution that is preferentially oriented perpendicular to the pump polarization. As a result, $\Delta\alpha_{\parallel}$ will show a residual bleaching while $\Delta\alpha_{\perp}$ shows a residual absorption, as is observed in the upper panel of Fig. 5.

An interesting question is at what stage of the relaxation the excited O–H oscillators show an increased orientational mobility. It is not likely that the O–H oscillators reorient faster while they are in the $v = 1$ state, as it was observed that the $1 \rightarrow 2$ transition shows in fact a slower reorientation than the $0 \rightarrow 1$ transition. [29]. Hence, the increased orientational mobility must be present in the intermediate state or in the ground state directly following the relaxation of the intermediate state. In either case, it seems likely that the increased mobility results from a transient high degree of excitation of local librational and hydrogen-bond stretching modes, as it can be expected that the excitation of these modes increases the orientational mobility of the O–H group. It has been shown that both scenarios can account for the experimental observations [35]. In case the increased mobility is associated with the intermediate state, a good description is obtained with a time constant $\tau_{\mathrm{or}} = 1.7$ ps in the intermediate state $v = 0^*$ and $\tau_{\mathrm{or}} = 3.2$ ps in the other states $v = 0$, $v = 1$, and $v = 0'$. Alternatively, a good description of the data is obtained by taking the anisotropy to decay by 14% directly following the relaxation to $v = 0'$. In that case τ_{or} is 3 ps for all

states. Which of the two scenarios is the most likely clearly depends on the precise character of the intermediate state $v = 0^*$.

With molecular dynamics simulations it was shown that the relaxation of the O–H stretch vibration of the HDO molecule most likely proceeds through the overtone of the bending mode [39,40]. The energy gap between the O–H stretch vibration and the overtone of the bending mode is $\sim$500 cm^{-1}, and this energy likely will be released in librational and hydrogen-bond modes. The subsequent relaxation of the intermediate state involves the release of the much larger energy of the overtone of the bending mode of $\sim$2900 cm^{-1}. Hence, if the relaxation indeed proceeds through the overtone of the bending mode, the increased mobility of the relaxing molecules most likely occurs after the relaxation of the intermediate state, as this relaxation is expected to result in the highest degree of excitation of intermolecular librational and hydrogen-bond modes.

The measured anisotropy can be corrected for the residual anisotropy of the ground state by subtraction of this latter contribution. The remaining signal represents the anisotropic signal of the excitation of the O–H stretch vibration only. This anisotropy is represented by the solid curve in Fig. 6a. It should be reminded that the O–D vibration does not at all show a residual anisotropy of the ground state following vibrational relaxation. Possible reasons for this difference are that the vibrational relaxation of the O–D vibration proceeds via a different mechanism and that, as a result of the lower frequency of the O–D vibration, the energy released in the relaxation is not sufficient to induce a significant increase of the orientational mobility of the O–D groups.

Average orientational dynamics in H_2O and D_2O

Figure 7 shows the anisotropy of the O–D stretch vibration of HDO dissolved in H_2O measured as a function of delay for a pump frequency of 2500 cm^{-1} and three different probe frequencies. The anisotropy signals shown are obtained by correcting the measured $\Delta\alpha_{\parallel}$ and $\Delta\alpha_{\perp}$ for the thermalization signal as determined from the isotropic data. An exponential fit

to the data shown in Fig. 7 yields a time constant τ_{or} of 2.5±0.2 ps at all probe frequencies, in agreement with earlier results [34,42].

The reorientation time constant of the OD vibration of HDO in H_2O (2.5±0.2 ps) is observed to be somewhat shorter than that of the OH vibration of HDO in D_2O (3±0.3 ps) [29–32]. At first sight it may seem surprising that the orientational relaxation of the O–D group proceeds faster than that of the O–H group, as its moment of inertia is almost twice as large. However, here it should be realized that there exist two regimes for the reorientation. On very short timescales (<200 fs), the O–H/O–D group can show a limited free rotation (libration) while keeping the donated hydrogen bond intact. This regime will be discussed in the following subsection. On longer timescales, which is of relevance here, the orientational dynamics of the O–H/O–D groups require rearrangements of the water network [1,2]. In this regime the orientational dynamics are no longer determined by the moment of inertia, but instead are governed by the relative motions of the water molecules and, in particular, by the dynamics of hydrogen-bond breaking and reformation. A good measure for the translational mobility of the water molecules is provided by the value of the viscosity. Using the viscosities of H_2O and D_2O (0.9 mPa s and 1.1 mPa s, respectively), the reorientation times of the O–H and O–D are estimated to show a ratio of 0.8, which is very similar to the measured ratio of the reorientation time constants. It should be noted that this finding does not imply that the orientational motion of the water molecules is diffusive. In fact, in a recent molecular dynamics study it was shown that the reorientation involves fast and large angular jumps between different hydrogen-bond configurations [1]. The scaling with the viscosity thus likely follows from the fact that the rate-limiting steps of the reorientation are formed by (translational) molecular motions of which the rate is well characterized by the viscosity.

The measured average molecular reorientation times of 2.5/3 ps in H_2O/D_2O agree well with the results obtained with other techniques. NMR studies also arrive at a reorientation time τ_{or} of the water molecule of 2.5 ps in liquid H_2O [7]. In comparing the results of femtosecond pump-probe and NMR with the results of dielectric relaxation studies and THz

absorption, it should be realized that these techniques measure different orientational correlation functions. Femtosecond pump-probe and NMR probe the second order correlation function $\langle P_2(\cos\theta(t))\rangle$, whereas the signal in dielectric relaxation and THz absorption spectroscopy is related to the first order correlation function $\langle P_1(\cos\theta(t))\rangle$. The ratio between the first and second order correlation times τ_1 and τ_2, is determined by the nature of the reorientation mechanism. In the case of pure (small step) rotational diffusion $\tau_1 = 3\tau_2$, but if the reorientation takes places via, for example, jump diffusion this ratio can be somewhat different [1].

In dielectric relaxation studies of liquid water, a main relaxation component with a time constant of 8.3 ps was found [10]. Similar values were found in THz spectroscopic studies of H_2O and D_2O. [11–13] At room temperature the correlation times of the slow component were determined to be 8.5 ps for H_2O and 10 ps for D_2O. When comparing these values with the second order correlation times (2.5 ps and 3 ps, respectively) one finds a ratio that is close to 3. In addition to the component with a time constant of 2.5/3 ps, dielectric relaxation and THz absorption studies report a weaker and much faster component with a time constant with a value on the order of 100 fs [11–13]. The origin of this fast component will be discussed in the following subsection.

A. Librational motions

In Figure 8 the anisotropy of the O–H stretch vibration of HDO:D_2O is shown as a function of delay in the time interval up to 1.5 ps [32] (courtesy of Andrei Tokmakoff). This measurement is performed with mid-infrared pulses with a pulse duration of 45 fs. The figure clearly shows that the anisotropy decay takes place on two distinctly different time scales. The anisotropy shows a rapid partial decay in the first 200 fs. Here it should be noted that the signals measured in Ref. [32] will show little contribution of coherent artifacts because the sample used in this study is a free-flowing water jet. The fast decay is followed by the much slower dominant decay component with a time constant of $\sim$3 ps [29–31].

The fast decay time is likely the result of the librational motion of the O–H group, i.e. the hindered rotation of the intact O–H$\cdots$O hydrogen-bonded system [32]. This interpretation was recently confirmed by a molecular dynamics study in which it was found that the librational motion indeed leads to a partial decay of the anisotropy in the first 200 fs [2]. The magnitude of this decay was calculated to be strongly dependent on the frequency of the O–H stretch vibration [2]. When the frequency increases, the hydrogen bond becomes weaker and the magnitude of the librational cone increases.

The angle of the librational cone can be estimated by assuming that the rotation over this cone leads to the delocalization of an the O–H/O–D dipole over a cone with semi-angle θ_0. As was shown by Lipari and Szabo [43] this leads to a decrease of the initial value of the anisotropy from 0.4 to

$$R(0) = \frac{2}{5}\left[\frac{1}{2}\cos\theta_0(1+\cos\theta_0)\right]^2 \tag{3}$$

In the experiment shown in Fig. 8 the O–H stretch absorption is pumped and probed with broadband infrared pulses. Therefore, the observed librational cone will represent an average over the whole absorption band. In Fig. 8, the fast process leads to a decay of the anisotropy to a value of 0.3, which corresponds to a semi-angle of free rotation of 25 °. This value is in excellent agreement with the calculated value of the librational cone of 24° at the center of the absorption band [2].

Frequency dependence of the reorientation?

Femtosecond pump-probe spectroscopy offers the possibility to distinguish the orientational dynamics of water molecules absorbing at different frequencies. In Fig. 7 results are presented in which the anisotropy decay is measured at three different probe frequencies in the absorption band of the O–D stretch vibration. At all three probe frequencies the same dynamics are observed, which agrees with the findings of previous studies of the anisotropy dynamics of the O–D stretch vibration of HDO dissolved in H_2O [33,34]. The absence of a

frequency dependence of the anisotropy decay suggests that the reorientation is a collective process that is not at all correlated with the strength of the local hydrogen bond [33].

Interestingly, in earlier studies of the orientational dynamics of the O–H stretch vibration of HDO dissolved in D_2O, a frequency-dependent anisotropy decay was observed [28–31]. In these studies the measured anisotropy showed an additional relatively fast component with a time constant of ∼700 fs in case the O–H absorption band was excited in the blue wing. It should be noted that this faster decay cannot be caused by the presence of a residual anisotropy in the ground state following the relaxation of the O–H stretch vibration. The effects of this residual anisotropy become apparent only for delays >2 ps, whereas the fast additional decay of the anisotropy is observed for delays <1.5 ps. The additional fast decay can also not be caused by librations. The partial decay of the anisotropy due to librations is nearly complete after 200 fs [2,32], whereas the dynamics observed in the blue wing of the O–H stretch vibration are much slower, having a time constant of $\sim$ 700 fs.

It is remarkable that the studies on HDO:H_2O and HDO:D_2O yield such different frequency dependencies. An important experimental difference between these studies is that in the studies of HDO:D_2O the pump was tuned together with the probe, while in the experiments on the O-D vibration, the pump was not tuned at all. In these latter studies the dynamics at different probe frequencies were obtained by spectrally dispersing the broadband probe pulse. Hence, the reported differences in frequency dependence may not be due to the isotopic character of the probed oscillator, but rather due to the dependence of the observed dynamics on the frequency of the excitation. To test this idea, we performed an experiment on the O–D stretch vibration of HDO:H_2O in which the pump pulse is tuned through the absorption band, and in which the dynamics are detected at a probe frequency that corresponds to the central frequency of the pump pulse. In Fig. 9 the thus measured anisotropy of the O–D stretch vibration is shown as a function of delay for four different pump and probe frequencies. When both pump and probe are tuned to the blue wing, the anisotropy of the O–D vibration shows indeed an additional rapid anisotropy decay, in agreement with the earlier observations for the O–H vibration [28,30,31].

B. Jumping water molecules

To study the origin of the 700 fs decay component in the anisotropy, we probe the spectral dependence of the anisotropy of the O–D stretch vibration of HDO dissolved in H_2O for two different pump frequencies and five different delays. The results are shown in Fig. 10. When the O–D stretch vibration is pumped close to its central frequency (upper panels), the anisotropy is nearly the same at all probe frequencies, except in the frequency region where the bleaching changes into an induced absorption. In this frequency region the signal results from the competition of these two signals which leads to an erratic behavior of the anisotropy. With increasing delay, the anisotropy decays shows the same decay dynamics at all probe frequencies. This finding agrees with the results shown in Fig. 7.

When the pump frequency is tuned to the blue wing of the absorption spectrum (lower panels of Fig. 10), the anisotropy is observed to become strongly frequency dependent in the first few picoseconds. An interesting observation is that the anisotropy in the center and the red wing is significantly lower than 0.4, already at a delay of 0.2 ps. This observation shows that directly after the excitation, the signals in the center and in the red wing contain a significant contribution of water molecules that have reoriented. This fast anisotropy decay cannot be due to librations, because librations lead to a fast partial anisotropy decay [32,2] of which the magnitude *decreases* with decreasing frequency [2], which is thus opposite to the results shown in Fig. 10. In Fig. 11 the dynamics of the anisotropy at different probe frequencies are shown following excitation in the blue wing of the absorption band. It is clearly seen that in the center and the red wing the anisotropy starts at a very low initial value, rises and then decays again with the long-time reorientation time constant of $\sim$2.5 ps.

The low value of the anisotropy in the center and the red wing following excitation in the blue wing (lower panels of Fig. 10) cannot be due to a high intrinsic reorientation rate of molecules absorbing in the center and the red wing. The upper panels of Fig. 10 clearly show that water molecules absorbing in the center and the red wing in fact show a slow

reorientation. Therefore, the large fraction of reoriented molecules in the center and the red wing *following excitation in the blue wing* must be due to excited molecules that reorient while jumping from the excited blue wing to the center and the red wing of the absorption band. This finding closely agrees with the molecular jump model for reorientation developed by Laage and Hynes [1]. In this model, the reorientation involves the breaking of the old hydrogen bond and the formation of a new hydrogen bond, which leads to a large and abrupt change in the frequency of the O–D vibration. In case the pump pulse is tuned to the blue wing of the absorption band, there will be few molecules directly excited in the center and the red wing of the absorption band. As a result, the relative contribution to the signal of molecules that have reoriented and jumped will be relatively large at these frequencies, leading to a low anisotropy already at early delays. A significant part of the frequency jumps takes place within 100 fs, as no initial fast anisotropy decay could be resolved in the center and the red wing of the absorption band. In the blue wing of the absorption band, the number of directly excited molecules is large and the *relative* contribution of molecules that have reoriented and have jumped to all possible frequencies in the absorption band will be small. Hence, in the blue wing the initial anisotropy is high.

We compare the data with calculated results obtained with a phenomenological model for the anisotropy dynamics that includes the spectral diffusion of liquid water [14–17,19–25,27,32]. The spectral diffusion of water has been shown to contain both slow and fast components. The slow component of the spectral diffusion has been modelled with a single time constant with a value of ∼1 ps [14–16,19–24,27,32] and with two time constants of ∼0.4 ps and ∼1.8 ps [25]. Here we describe the slow component of the spectral diffusion as a gaussian spectral diffusion process (weak frequency modulation limit) with an exponentially decaying frequency correlation function $\langle \delta\nu(t)\delta\nu(0)\rangle = \mathrm{e}^{-t/\tau_c}$ with a time constant τ_c of 700 fs. Regarding the fast spectral diffusion two components can be distinguished. The first component is of gaussian nature (weak modulation limit), and leads to a broadening that is close to the motional narrowing limit. This component is included in the model via the homogeneous linewidth, which is a correct approach as the time resolution of our experiment

is ∼200 fs. We use a value of 80 cm^{-1} for this linewidth [21]. The other fast component is a spectral diffusion process in which the frequency jumps are of large amplitude leading to a complete loss of correlation to the frequency before the jump (strong frequency modulation limit=non-gaussian). This component is only observed for molecules absorbing in the blue wing of the spectrum [26,27]. The jump in frequency has been assigned to the return of a hydroxyl group in a non-hydrogen-bonded configuration to a hydrogen-bonded configuration [27]. The non-hydrogen-bonded configuration is likely a species in which the water molecule forms a weak bifurcated hydrogen bond to two water molecules. The formation of this bifurcated configuration probably involves the gradual approach of a new hydrogen-bonded partner and the weakening and bending of the hydrogen bond to the original hydrogen-bonded partner. The return from the bifurcated state to a single strong hydrogen bond can be both due to the reformation of the original hydrogen bond, or due to the formation of a hydrogen bond to the new partner, i.e. a switching event [1,27].

In case the evolution through the bifurcated state leads to the formation of a new hydrogen bond, hydroxyl group has reoriented. Laage and Hynes show that in this case the O–H group has rotated over ∼60° [1]. This angle is quite close to the magic angle of 54.7°. Therefore, in the model we assume that the switching to a new hydrogen-bonded partner leads to a complete decay of the anisotropy. It is further assumed that switching occurs in 50% of the fast and strong spectral modulation events. The frequency dependence of the fast spectral diffusion component is described with a phenomenological expression that is fitted to the experimental results of Figs. 7, 9, 10, and 11. This expression is given in Appendix B. The calculated results are shown in the right hand panels of Fig. 10, and are represented by the solid curves in Figs. 7, 9, and 11. The calculated results are in excellent agreement with the data.

I. DISCUSSION

In Fig. 7 and Refs. [33–35] it is observed that the anisotropy decay does not depend on frequency when the absorption band is pumped at its central frequency. This can now be explained as follows. In case the absorption band is pumped in the center, there will be little direct excitation of rapidly reorienting/spectrally jumping molecules. As a result, the anisotropy will be close to 0.4 (librations not considered), and will be the same for all frequencies. The slow spectral diffusion will lead to an ongoing production of blue-shifted molecules. The reorientation and subsequent frequency jumping of these molecules through the absorption band lead to the same decay of the anisotropy at all frequencies with a time constant of 2.5 ps.

The accelerated initial decay of the anisotropy that is observed when water molecules are pumped and probed in the blue wing of the absorption band (Fig. 9) can now also be explained. In the earlier studies of the anisotropy dynamics of the O–H stretch vibration of HDO dissolved in D_2O, the fast initial decay in the blue wing was assigned to a faster intrinsic reorientation of water molecules that remain in the blue wing [29,28,30,31]. We find now that this interpretation is not correct because it is inconsistent with the additional observation that the excitation in the blue wing leads to a very rapid decay of the anisotropy in the center and the red wing of the absorption band. The reorientation leads to a complete loss of memory of the frequency of the water molecule. This loss of memory implies that the reoriented molecules can be found equally distributed over the absorption band. Hence, the faster initial anisotropy decay in the blue wing of the spectrum is *not* the result of a fast accumulation of reoriented molecules at these particular frequency positions. Instead, in the case of excitation in the blue wing, the *relative* contribution of reoriented molecules to the signal in the blue wing will in fact be *lower*, leading to a higher initial anisotropy. At later delay times, the anisotropy at different frequencies will be equilibrated as a result of the slow spectral diffusion process with a time constant of $\sim$700 femtoseconds. This equilibration of the high initial anisotropy at the blue side with the lower anisotropy signals

at lower frequencies implies that the anisotropy in the blue wing explains the accelerated decay with a time constant [28–30] that is very similar to the average time constant of the spectral diffusion of 700 fs [19,20,22,25,32].

The jumping mechanism for reorientation offers an alternative explanation for the fast decay (<200 fs) of the anisotropy shown in Fig. 8 that was assigned to librations. In the case of broadband excitation, part of the excited molecules will directly undergo reorientation and frequency jumping, thereby leading to a fast partial decay of the anisotropy at all frequencies. Hence, the fast initial decay shown in Fig. 8 could in fact represent the rapid reorientation and jumping of the fraction of the molecules that are excited by the blue wing of the spectrum of the pump pulse. It will be difficult to discriminate experimentally between this alternative explanation for the fast initial decay and the explanation in terms of librations, because for both explanations the amplitude of the fast initial decay increases when the excitation pulse is tuned to the blue wing of the absorption band.

The experimental observations shown in Figs. 8-12 are largely consistent with the recently reported molecular jumping mechanism for reorientation of liquid water by Laage and Hynes [1,2]. However, there is also a significant difference between the experimental results and this theory. According to the theoretical work the probability of a water molecule to evolve to the bifurcated transition state for reorientation should not be dependent on frequency [2]. This prediction is not confirmed by the experimental observations that show a clear dependence of the anisotropy dynamics on the excitation frequency (Figs. 10 and 11). The theoretical prediction also does not agree with the observation in 2D-IR studies that excitation in the blue wing leads to a rapid frequency jumping, while excitation in the center and the red wing does not lead to such an effect [26,27]. The experimental results thus indicate that the molecular dynamics simulations of Refs. [1,2] underestimate the correlation between the frequency of the O–H/O–D oscillator and the jumping probability.

The large jumping probability in the blue wing of the spectrum is probably not the result of a direct excitation of molecules in the bifurcated transition state, as this state is likely extremely short-lived [1,2,27]. Therefore, the transition state configuration itself will

contribute negligibly to the absorption, even in the blue wing of the absorption band. In view of the above, the frequency dependence of the jumping probability has to result from the fact that molecules absorbing in the blue wing have a higher probability to evolve to the transition state: for water molecules with long and/or bent hydrogen bonds the approach of a second hydrogen-bond partner will be easier and more frequent than for water molecules with short and straight hydrogen bonds.

CONCLUSIONS

We present and discuss the work on the molecular reorientation of liquid water performed with polarization-resolved femtosecond mid-infrared spectroscopy. In these experiments, the reorientation dynamics is probed by measuring the anisotropy dynamics of the excitation of the O–H or O–D stretch vibration of isotopically diluted water. An advantage of femtosecond mid-infrared spectroscopy over other techniques is that the tuning of the excitation and probing frequency the technique allows in principle for the distinct measurement of the dynamics of different sub-ensembles of water molecules.

The experiments and recent theoretical work [1,2] show that the molecular reorientation of liquid water results from a fraction of the molecules that absorb in the blue wing of the spectrum and that show long and weak hydrogen bonds. These molecules can evolve to a state in which the O–H/O–D group is engaged in a double, bifurcated hydrogen-bond with two other water molecules. The breaking of one of these bonds and the contraction of the other leads to a large change in frequency of the O–H/O–D. If the evolution through the bifurcated state leads to the formation of a hydrogen bond with a new partner (switching event), this leads to an effective rotation of the O–H/O–D group over $\sim 60^\circ$ [1]. The rapid change in frequency following excitation in the blue wing has also been observed in recent vibrational correlation echo measurements of the spectral dynamics of isotopically diluted water [26,27]. The anisotropy measurements show that the probability to evolve to the transition state for reorientation/frequency jumping strongly depends on frequency, this

process more likely to occur in the blue wing than in the center and the red wing of the absorption band. This frequency dependence constitutes a difference with in the theoretical work by Laage and Hynes in which it was found that this probability would not be dependent on frequency [2].

The spectral dynamics of the anisotropy can be accurately described with a model that includes both the frequency jumping and the slow gaussian (weak frequency modulation limit) spectral diffusion of liquid water. In case the absorption band is pumped in the center, as was the case in the previous studies of the orientational dynamics of the O–D vibration [33–35], there will be little direct excitation of rapidly reorienting/spectrally jumping molecules. As a result, the initial anisotropy will be close to 0.4 and will be the same for all frequencies. The reorientation results from the molecules that slowly diffuse to the blue and then undergo a reorientation and frequency jump through the absorption band. This process leads to the same decay of the anisotropy at all frequencies with a time constant of 2.5 ps. In the case of excitation in the blue wing, the rapid frequency jumps cause the early-time value of the anisotropy to show a strong decrease with decreasing frequency. The subsequent exchange of the anisotropy at different frequencies due to the slow spectral diffusion process ($\sim$700 fs), leads to an additional partial decay of the anisotropy in the blue wing with a similar time constant. After the spectral equilibration is complete, the anisotropy shows again the same decay at all frequencies with a time constant of $\sim$2.5 ps.

ACKNOWLEDGMENT

The research presented in this paper is part of the research program of the Stichting Fundamenteel Onderzoek der Materie (Foundation for Fundamental Research on Matter) and was made possible by financial support from the Nederlandse Organisatie voor Wetenschappelijk Onderzoek (Netherlands Organization for the Advancement of Research).

APPENDIX A: RELAXATION MODEL

The delayed thermalization can be accounted for by introducing an intermediate level in the relaxation of O–H/O–Dvibration. As a result, the energy of the OH-stretch vibration is not directly converted into heat but is first transferred to an intermediate level. The subsequent decay of the intermediate level leads to the thermal population of low-frequency modes. The model is illustrated in Fig. 4. The decay of the O–H/O–D stretch vibration occurs with a time constant τ_1 and that of the intermediate level with a time constant τ_*. The following equations describe the dynamics of the molecules that are excited by the pump pulse:

$$\begin{aligned} \frac{dN_1}{dt} &= -k_1 N_1, \\ \frac{dN_0^*}{dt} &= k_1 N_1 - k_* N_0^*, \\ \frac{dN_0'}{dt} &= k_* N_0^*. \end{aligned} \tag{4}$$

These equations can be integrated to yield the following expressions for the populations,

$$\begin{aligned} N_1(t)/N_1(0) &= e^{-k_1 t}, \\ N_0^*(t)/N_1(0) &= \frac{k_1}{k_* - k_1}\left(e^{-k_1 t} - e^{-k_* t}\right), \\ N_0'(t)/N_1(0) &= \frac{k_1}{k_* - k_1} e^{-k_* t} - \frac{k_*}{k_* - k_1} e^{-k_1 t} + 1. \end{aligned} \tag{5}$$

The time-dependent absorption change that results from the populations of the different levels is given by:

$$\begin{aligned} \Delta\alpha_{\mathrm{iso}}(\omega, t) &= N_1(t)\sigma_{12}(\omega) - \left[N_1(0) + N_1(t)\right]\sigma_{01}(\omega) + \\ &\quad N_0^*(t)\sigma_{01}^*(\omega) + N_0'(t)\sigma_{01}'(\omega) \\ &= N_1(t)\sigma_{12}(\omega) + \left[-N_1(0) - N_1(t) + N_0^*(t) + N_0'(t)\right]\sigma_{01}(\omega) + \\ &\quad N_0^*(t)\Delta\sigma_{01}^*(\omega) + N_0'(t)\Delta\sigma_{01}'(\omega), \end{aligned} \tag{6}$$

where $\sigma_{01}(\omega)$ is the ground state spectrum, $\sigma_{01}(\omega)^*$ is the spectrum of the intermediate state, $\sigma_{01}'(\omega)$ is the spectrum of the ground state after thermalization of the pump energy,

and $\sigma_{12}(\omega)$ is the excited state spectrum. The cross-section differences $\Delta\sigma^*_{01}(\omega)$ and $\Delta\sigma'_{01}(\omega)$ are given by $\Delta\sigma^*_{01}(\omega) = \sigma^*_{01}(\omega) - \sigma_{01}(\omega)$ and $\Delta\sigma'_{01}(\omega) = \sigma'_{01}(\omega) - \sigma_{01}(\omega)$. The change in cross-section following thermalization is related to the absorption change at large delays $\Delta\alpha_{\mathrm{f}}(\omega)$ by:

$$\Delta\alpha_{\mathrm{f}}(\omega) = N_1(0)\Delta\sigma'_{01}(\omega). \tag{7}$$

Substitution of equation (7) in equation (7) yields:

$$\Delta\alpha_{\mathrm{iso}}(\omega,t) = N_1(t)\sigma_{12}(\omega) + \left[-N_1(0) - N_1(t) + N_0^*(t) + N_0'(t)\right]\sigma_{01}(\omega) \tag{8}$$

$$+ \quad N_0^*(t)\Delta\sigma^*_{01}(\omega) + \frac{N_0'(t)}{N_1(0)}\Delta\alpha_{\mathrm{f}}(\omega). \tag{9}$$

Substituting the expressions for the populations into this equation, we obtain:

$$\begin{aligned}\Delta\alpha_{\mathrm{iso}}(\omega,t) = {} & N_1(0)\left[\sigma_{12}(\omega) - 2\sigma_{01}(\omega)\right]e^{-k_1 t} + \\ & N_1(0)\Delta\sigma^*_{01}(\omega)\frac{k_1}{k_* - k_1}(e^{-k_1 t} - e^{-k_* t}) + \\ & \Delta\alpha_{\mathrm{f}}(\omega)\left\{\frac{k_1}{k_* - k_1}e^{-k_* t} - \frac{k_*}{k_* - k_1}e^{-k_1 t} + 1\right\}.\end{aligned} \tag{10}$$

The first term of the last expression represents the bleaching of the fundamental transition and the absorption of the excited $v = 1$ state. The second term represents the change in absorption associated with the occupation of the intermediate state, and the third term represents the change in absorption resulting from the thermalization.

APPENDIX B: KINETIC MODEL FOR ANISOTROPY DYNAMICS

The spectral diffusion and the reorientation dynamics are calculated using a Brownian oscillator model. In this model, the spectral dynamics of the $v = 0 \rightarrow 1$, $v = 1 \rightarrow 0$ and $v = 1 \rightarrow 2$ transitions are described using displaced but otherwise equivalent harmonic potentials in a low-frequency coordinate, in this case the donated O–H$\cdots$O/O–D$\cdots$O hydrogen bond. The potential energy is given by:

$$V(r) = a(r - r_v)^2 \tag{11}$$

with $V(r)$ the energy in J, $a = 10.68e - 24\text{J/pm}^2$, r and r_0 the hydrogen-bond length in pm (=10^{-12} m). To obtain the energy $V(r)$ in cm^{-1}, a has to be multiplied by $1/(100ch)$, with c the velocity of light in m/s, and h Planck's constant. The value of r_v depends on the vibrational state v: $r_0 = 285$ pm (=1×10^{-12} m), $r_1 = 280.5$ pm, and $r_2 = 276$ pm. Since the potential energy curves are parabolic, the transition frequency depends linearly on the hydrogen-bond coordinate r. The transition frequency $\nu_{v\rightarrow v+1}(r)$ in $\text{cm}^{-1} = \nu_{0,v\rightarrow v+1} + 4.8(r-r_v)$, with r and r_v defined in pm and $\nu_{0,v\rightarrow v+1}$ the transition frequency at the minimum of the potential energy curve v.

The hydrogen-bond coordinate is divided into bins that each correspond to a particular length interval, namely 1 pm, of the hydrogen bond. The slow stochastic gaussian spectral diffusion and the fast non-gaussian frequency jumping process lead to an exchange of population between the bins. The gaussian spectral diffusion is described in the following way. In each time step of the integration, the bins exchange population with their next-nearest neighbors with a time constant that is given by:

$$k_s = \begin{cases} k_h e^{-\Delta V/k_\text{B}T} & \Delta V > 0 \\ k_h & \Delta V < 0 \end{cases}, \tag{12}$$

with ΔV the difference in potential energy at the central positions of the bins. Eventually this population exchange process results in a Boltzmann distribution. which for the harmonic potential V_0 corresponds to a Gaussian distribution in the position coordinate r around r_0. The rate constant k_h is related to the autocorrelation time constant τ_c via $1/k_h = \tau_c(1-\gamma)$ [48]. The parameter γ depends on the width of the gaussian equilibrium distribution : $\gamma^2 = 1-4/w^2$, with w the half width at 1/e of the maximum of the equilibrium distribution. w was equal to 19.5 pm, and thus γ=0.9947 and $1/k_h$=3.7 fs. The large value of γ implies that the stochastic modulation of the hydrogen-bond length is correctly modelled as a Gaussian process, since the change in hydrogen-bond length r resulting from a single modulation event is small compared to the width of the Gaussian distribution in r [48].

The fast frequency jumping is described as an additional population transfer process in which the population is redistributed over the whole absorption band. The time constant of this transfer depends on the length of the hydrogen bond:

$$k_{\mathrm{j}}(r) = \frac{A}{1 + e^{-b(r-r_j)}}, \tag{13}$$

A fit to the experimental data of Figs. 7, 8, 10 and 11 yields A=0.5×10^{13} s^{-1}, $b = 0.5$, and $r_j = 294$ pm. These parameters are the only fit parameters in the model. At every time step this process leads to a loss of population that depends on the length r, and a gain of population that is assumed to show the same dependence on r as the thermal population distribution. Hence, the jumping process will effectively lead to a transfer of population from the bins at large values of r to all other bins, with most of the population being transferred to the bins that are close to the minimum of the potential.

The anisotropy decay is calculated by defining anisotropic and isotropic population changes $\Delta n_{v,\mathrm{ani}}(r,t)$ and $\Delta n_{v,\mathrm{iso}}(r,t)$ in the potentials of $v = 0$ and $v = 1$. The anisotropic population change is defined as the population change probed by a probe pulse with a polarization parallel to that of the pump, minus the population probed with a probe pulse with perpendicular polarization. The excitation by the pump pulse, which is assumed to be a gaussian with a pulse duration of 0.2 ps, results in holes $\Delta n_{0,\mathrm{ani}}(r,t)$ and $\Delta n_{0,\mathrm{iso}}(r,t)$ in the population distribution of $v = 0$, and to induced population distributions $\Delta n_{1,\mathrm{iso}}(r,t)$ and $\Delta n_{1,\mathrm{ani}}(r,t)$ in $v = 1$. The r dependence of these population changes follows from the central frequency and the spectral width of the pump pulse, and the homogeneous line width. For the homogeneous line width we use Lorentzian with a full-width-at-half-maximum of 80 cm^{-1} [21].

The frequency fluctuation processes lead to an exchange of population between the bins. In the slow stochastic process both the isotropic and the anisotropic populations are conserved. In the fast frequency jumping process, only the isotropic population is conserved, the anisotropic population will decay. The frequency jump can both result from the reformation of the original hydrogen bond and from the formation of a new hydrogen bond

[1,2]. In the calculations we assume that half of the frequency jumps leads to a decay the anisotropy. The population changes $\Delta n_{v,\mathrm{ani}}(r,t)$ and $\Delta n_{v,\mathrm{iso}}(r,t)$ are calculated at all times using a fourth-order Runge-Kutta algorithm.

To calculate the isotropic and anisotropic signals as a function of frequency, the position- and time-dependent $\Delta n_{0,\mathrm{iso}}(r,t)$ and $\Delta n_{0,\mathrm{ani}}(r,t)$ are translated into frequency-dependent absorption changes $\Delta\alpha_{0\rightarrow1,\mathrm{iso}}(\nu,t)$, and $\Delta\alpha_{0\rightarrow1,\mathrm{ani}}(\nu,t)$, and $\Delta n_{1,\mathrm{iso}}(r,t)$ and $\Delta n_{1,\mathrm{ani}}(r,t)$ are translated into $\Delta\alpha_{1\rightarrow0,\mathrm{iso}}(\nu,t)$, $\Delta\alpha_{1\rightarrow0,\mathrm{ani}}(\nu,t)$, $\Delta\alpha_{1\rightarrow2,\mathrm{iso}}(\nu,t)$, and $\Delta\alpha_{1\rightarrow2,\mathrm{ani}}(\nu,t)$. Here it should be noted that the relation between r and the frequency of the transitions $v=0\rightarrow1$ and $v=1\rightarrow0$ differs from that between r and the frequency of the transition $v=1\rightarrow2$. Finally, the frequency- and time-dependent anisotropy R is obtained from:

$$R(\nu,t)=\frac{\Delta\alpha_{0\rightarrow1,\mathrm{ani}}(\nu,t)+\Delta\alpha_{1\rightarrow0,\mathrm{ani}}(\nu,t)-\Delta\alpha_{1\rightarrow2,\mathrm{ani}}(\nu,t)}{\Delta\alpha_{0\rightarrow1,\mathrm{iso}}(\nu,t)+\Delta\alpha_{1\rightarrow0,\mathrm{iso}}(\nu,t)-\Delta\alpha_{1\rightarrow2,\mathrm{iso}}(\nu,t)} \tag{14}$$

REFERENCES

[1] Laage, D.; Hynes, J. T. *Science* **2006**, *311*, 832.

[2] Laage, D.; Hynes, J. T. *Chem. Phys. Lett.* **2006**, *433*, 80 (2006).

[3] Woutersen, S.; Bakker, H. J. *Nature* **1999**, **402**, 507.

[4] Lock, A. J.; Bakker, H. J. *J. Chem. Phys.* **2002**, *117*, 1708.

[5] Cowan, M. L.; Bruner, B. D.; Huse, N.; Dwyer, J. R.; Chugh, B.; Nibbering, E. T. J.; Elsaesser, T.; Miller, R. J. D.; *Nature* **2005**, *434*, 199.

[6] Deak, J. C.; Pang, Y.; Sechler, T. D.; Wang, Z.; Dlott, D. D. *Science* **2004** *306*, 473.

[7] Smith, D. W. G.; Powles, J. G. *Mol. Phys.* **1966**, *10*, 451.

[8] Godralla, B. C.; Zeidler, M. D. *Mol. Phys.* **1986** *59*, 817.

[9] Hardy, E. H.; Zygar, A.; Zeidler, M. D.; Holz, M.; Sacher F. D. *J. Chem. Phys.* **2001**, *114*, 3174.

[10] Barthel, J.; Bachhuber, K.; Buchner, R.; Hetzenauer, H. *Chem. Phys. Lett.* **1990**, *165*, 369.

[11] Kindt, J. T.; Schmuttenmaer, C. A. *J. Phys. Chem.* **1996**, *100*, 10373.

[12] Rnne, C.; Thrane, L.; strand, P.-O.; Wallqvist, A.; Mikkelsen, K. V.; Keiding, S. R. *J. Chem. Phys.* **1997**, *107*, 5319.

[13] Rnne C.; strand, P.-O.;, Keiding, S. R. *Phys. Rev. Lett.* **1999**, *82*, 2888.

[14] Rey, R.; Moller, K. B.; Hynes, J. T. *J. Phys. Chem. A* **2002**, *106*, 11993.

[15] Lawrence, C. P.; Skinner, J. L. *J. Chem. Phys.* **2003** *118*, 264.

[16] Corcelli, S. A.; Lawrence, C. P.; Skinner, J. L. *J. Chem. Phys.* **2004**, *120*, 8107.

[17] Auer, B.; Kumar, R.; Schmidt, J. R.; Skinner, J. L. *Proc. Natl. Acad. Sci. USA* **2007**,

104,14215.

[18] Laenen, R.; Rauscher, C.; Laubereau, A. *Phys. Rev. Lett.* **1998**, *80*, 2622.

[19] Gale, G. M.; Gallot, G.; Hache, F.; Lascoux, N.; Bratos, S.; Leicknam, J.-C. *Phys. Rev. Lett.* **1999**, *82*, 1086.

[20] Woutersen, S.; Bakker, H. J. *Phys. Rev. Lett.* **1999**, *83*, 2077.

[21] Stenger, J.; Madsen, D.; Hamm, P.; Nibbering, E. T. J.; Elsaesser, T. *Phys. Rev. Lett.* **2001** *87*, 027401.

[22] Stenger, J.; Madsen, D.; Hamm, P.; Nibbering, E. T. J.; Elsaesser, T. *J. Phys. Chem. A* **2002**, *106*, 2341.

[23] Yeremenko, S.; Pshenichnikov, M. S.; Wiersma, D. A. *Chem. Phys. Lett* **2003**, *369*, 107.

[24] Fecko, C. J.; Eaves, J. D.; Loparo, J. J.; Tokmakoff, A.; Geissler, P. L. *Science* **2003**, *301*, 1698.

[25] Asbury, J. B.; Steinel, T.; Stromberg, C.; Corcelli, S. A.; Lawrence, C. P.; Skinner, J. L.; Fayer, M. D. *J. Phys. Chem. A* **2004**, *108*, 1107.

[26] Steinel, T.; Asbury, J. B.; Corcelli, S. A.; Lawrence,C. P.; Skinner, J. L.; Fayer, M. D. *Chem. Phys. Lett.* **2004**, *386*, 295.

[27] Loparo, J. J.; Roberts, S. T.; Tokmakoff, A. *J. Chem. Phys.* **2006**, *125*, 194522.

[28] Woutersen, S.; Emmerichs, U.; Bakker, H. J. *Science* **1997**, *278*, 658.

[29] Nienhuys, H.-K.; van Santen, R. A.; Bakker, H. J. *J. Chem. Phys.* **2000** *112*, 8487.

[30] Bakker, H. J.; Woutersen, S.; Nienhuys, H.-K. *Chem. Phys.* **2000**, *258*, 233.

[31] Gallot, G.; Bratos, S.; Pommeret, S.; Lascoux, N.; Leicknam, J.-C.; Kozinski, M.; Amir, W.; Gale, G. M. *J. Chem. Phys.* **2002**, *117*, 11301.

[32] Fecko, C. J.; Loparo, J. J.; Roberts, S. T.; Tokmakoff, A. *J. Chem. Phys.* **2005**, *122*, 054506.

[33] Steinel, T.; Asbury, J. B.; Zheng, J.; Fayer, M. D. *J. Phys. Chem. A* **2004**, *108*, 10957.

[34] Rezus Y. L. A.; Bakker, H. J. *J. Chem. Phys.* **2005**, *123*, 114502.

[35] Rezus Y. L. A.; Bakker, H. J. *J. Chem. Phys.* **2006**, *125*, 144512.

[36] Graener, H.; Seifert, G.; Laubereau, A. *Chem. Phys. Lett.* **1990**, *172*, 435.

[37] Timmer, R. L. A.; Bakker, H. J. *J. Chem. Phys.* **2007**, *126*, 154507.

[38] Schmidt, J. R.; Corcelli, S. A.; Skinner, J. L. *J. Chem. Phys.* **2005**, *123*.

[39] Rey, R.; Hynes J. T. *J. Chem. Phys* **1996**, *104*, 2356.

[40] Lawrence C. P.; Skinner, J. L. *J. Chem. Phys.* **2003**, *119*, 1623.

[41] Tan, H-S.; Piletic, I. R.; Fayer, M. D. *J. Chem. Phys.* **2005**, *122*, 174501.

[42] Piletic, I. R.; Moilanen, D. E.; Spry, D. B.; Levinger, N. E.; Fayer, M. D. *J. Phys. Chem.* **2006**, *110*, 4985.

[43] Lipari, G.; Szabo, A. *Biophys. J.* **1980**, *30*, 489.

[44] Wernet, P.; Nordlund, D.; Bergmann, U.; Cavalleri, M.; Odelius, M.; Ogasawara, H.; Naslund, L .-A.; Hirsch, T. K.; Ojamae, L.; Glatzel, P.; Pettersson, L. G. M.; Nilsson, A. *Science* **2004**, *304*, 996.

[45] Nilsson, A.; Wernet, P.; Nordlund, D.; Bergmann, U.; Cavalleri, M.; Odelius, M.; Ogasawara, H.; Naslund, L .-A.; Hirsch, T. K.; Ojamae, L.; Glatzel, P.; Pettersson, L. G. M. *Science* **2005**, *308*, 793.

[46] Smith, J. D.; Cappa, C. D.; Wilson, K. R.; Messer, B. M.; Cohen, R. C.; Saykally, R. J. *Science* **2004**, *306*, 851.

[47] Smith, J. D.; Cappa, C. D.; Messer, B. M.; Cohen, R. C.; Saykally, R. J. *Science* **2005**, *308*, 793.

[48] Burshtein A. I.; Malinovsky V. S. *J. Opt. Soc. Am. B* **1991**, *8*, 1098.

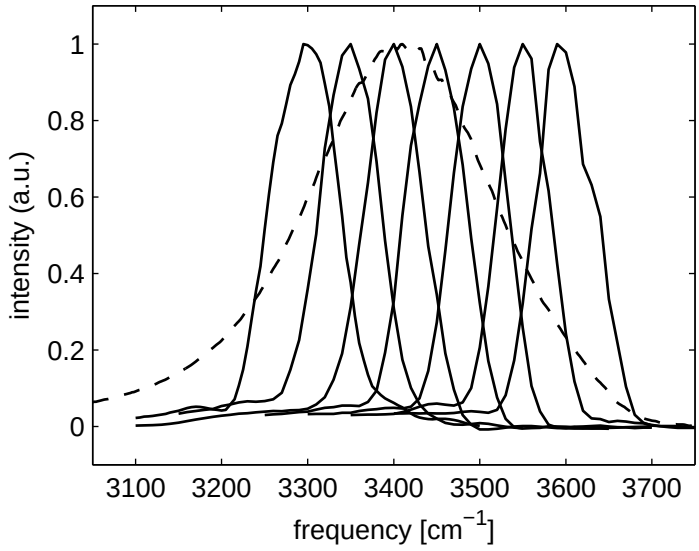

FIG. 1. Typical excitation spectra that are resonant with the O–H stretch vibration of a solution of 1% HDO dissolved in D_2O. For comparison also the linear absorption spectrum of the O–H stretch vibration is shown (dashed curve).

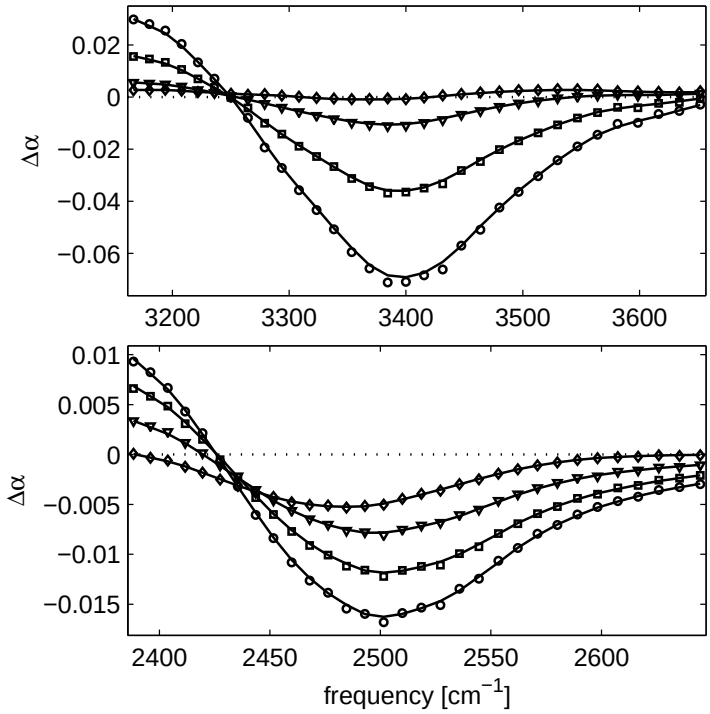

FIG. 2. Absorption change as a function of frequency induced by a pump pulse at 3400/2500 cm^{-1} (upper/lower panel) exciting the O–H/O–D stretch vibration of HDO dissolved in D_2O/H_2O. Shown are spectra at delays of 0.5 ps (circles), 1 ps (squares), 2 ps (triangles) and 4 ps (diamonds) between pump and probe. The solid lines represent the results of a fit of the data to the model described in Appendix A.

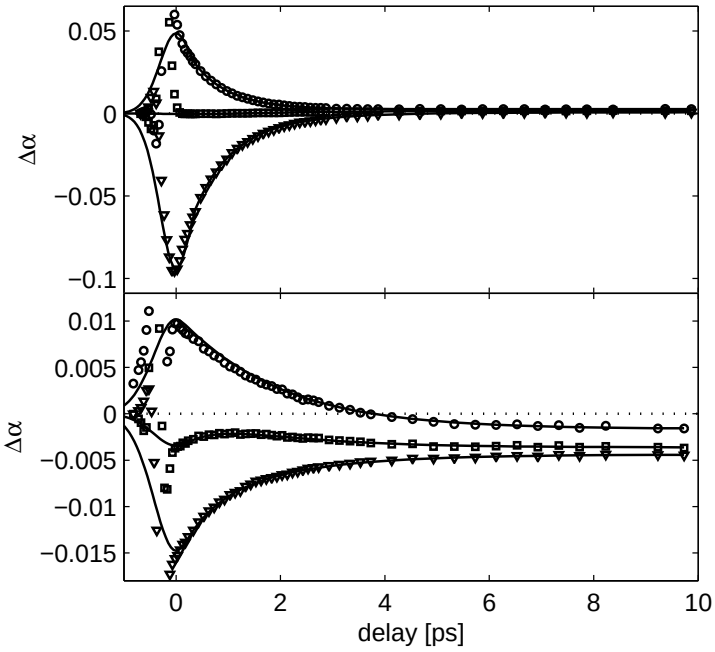

FIG. 3. Absorption change as a function of delay between pump and probe for a pump pulse at 3400/2500 cm^{-1} (upper/lower panel) exciting the O–H/O–D stretch vibration of HDO dissolved in D_2O/H_2O. Shown are transients for probe frequencies of 3170/2380 cm^{-1} (circles), 3250/2430 cm^{-1} (squares) and 3400/2480 cm^{-1} (triangles). The solid lines represent the results of a fit of the data to the model described in Appendix A.

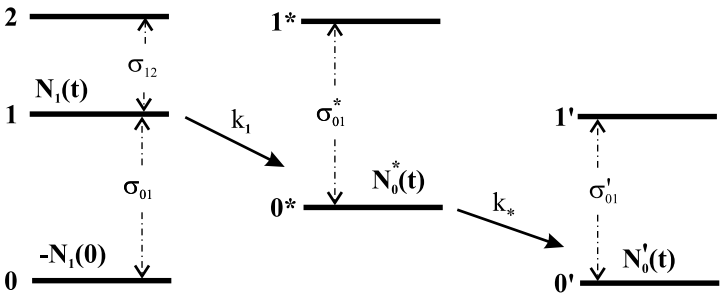

FIG. 4. Relaxation scheme of the O–H stretch vibration of HDO dissolved in D_2O and of the O–D vibration of HDO dissolved in H_2O. In the first step of the relaxation the population is transferred from $v = 1$ to an intermediate level $v = 0^*$. In the second step the intermediate level relaxes to the heated ground state $v = 0'$.

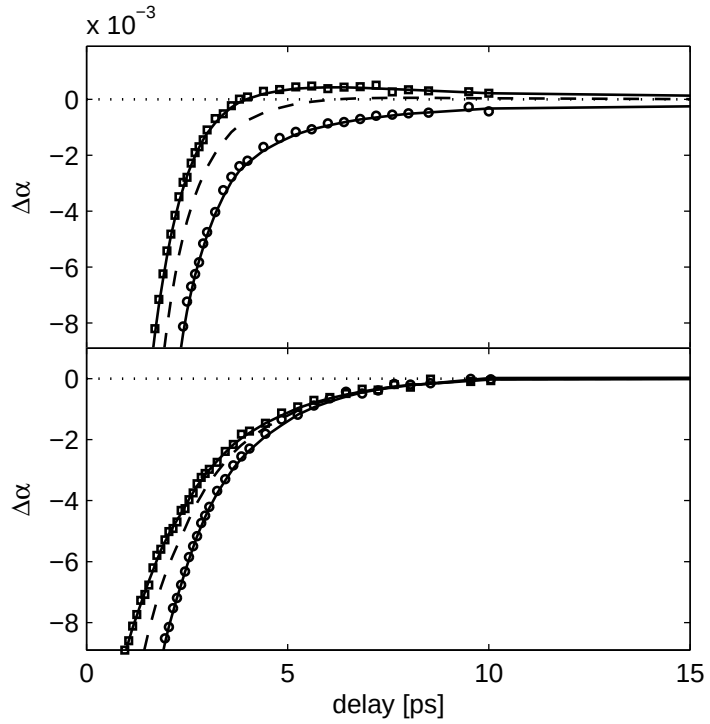

FIG. 5. Enlarged parallel (circles) and perpendicular (squares) probing signals measured with a pump pulse at 3400/2500 cm^{-1}(upper/lower panel) exciting the O–H/O–D stretch vibration of HDO dissolved in D_2O/H_2O. The signals are probed at frequencies of 3400/2500 cm^{-1}. The dashed lines represent the isotropic signals $((\Delta\alpha_{\parallel} + 2\Delta\alpha_{\perp})/3)$.

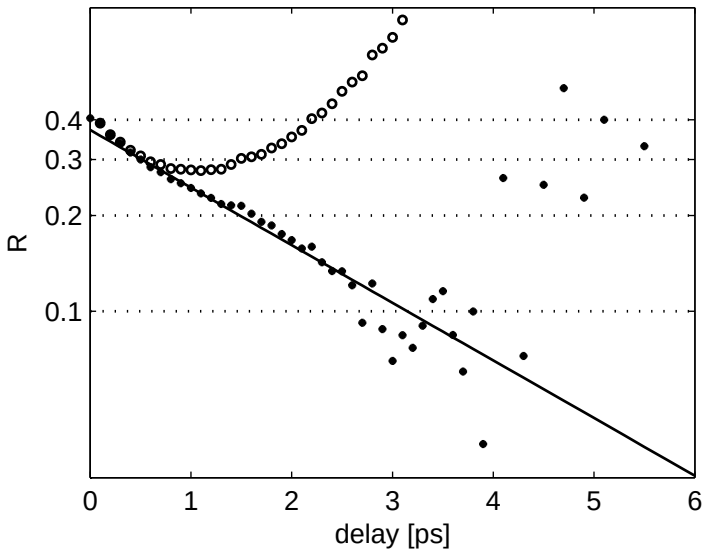
0.4
0.3
0.2
0.1
R
0
1
2
3
4
5
6
delay [ps]

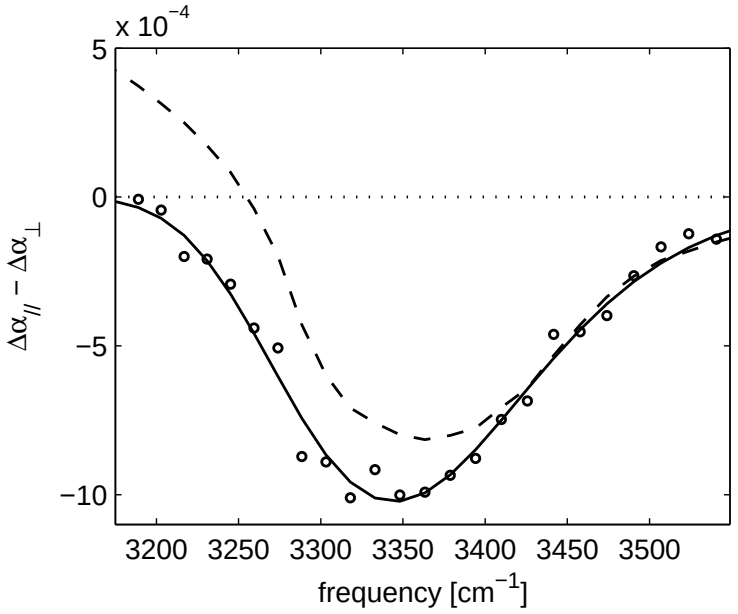
x 10^−4
5
0
−5
−10
Δα// − Δα⊥
3200
3250
3300
3350
3400
3450
3500
frequency [cm^−1]

FIG. 6. Fig. a: Anisotropy decay as a function of pump-probe delay for the O–H stretch vibration after subtraction of the heating effect (open circles) and after subtraction of the heating effect and correction for the anisotropy of the ground state that results from the relaxation of the O–H stretch vibration (filled circles). The solid line represents an exponential fit with a time constant of 3±0.2 ps. Fig. b: Difference between the parallel and perpendicular probing signals (circles, solid curve) measured for the O–H stretch vibration of HDO in D_2O at a delay of 3 ps. This difference signal represents a bleaching at all frequencies, in contrast to the early-time pump-probe signal measured at a delay of 0.3 ps (dashed line).

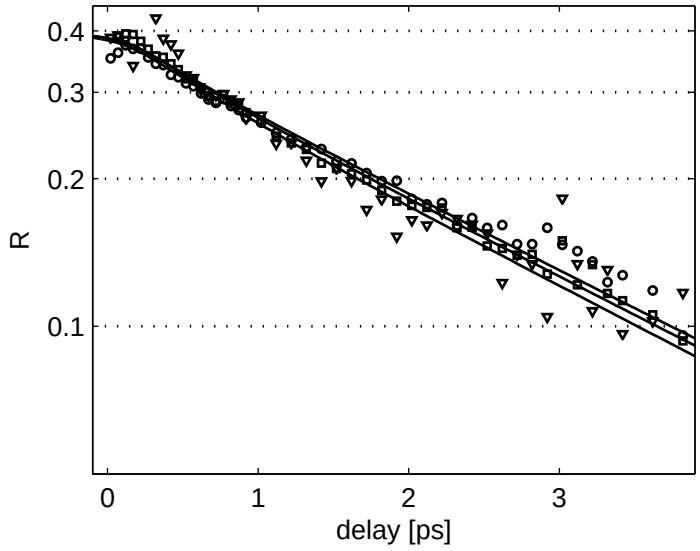

FIG. 7. Anisotropy of the O–D stretch vibration of HDO dissolved in H_2O as a function of delay between pump and probe for a pump frequency of 2500 cm^{-1}, and probe frequencies of 2500 cm^{-1} (circles), 2550 cm^{-1} (squares) and 2600 cm^{-1} (triangles). The points denote the experimental data, the solid lines represent the results of calculations performed with the model described in Appendix B.

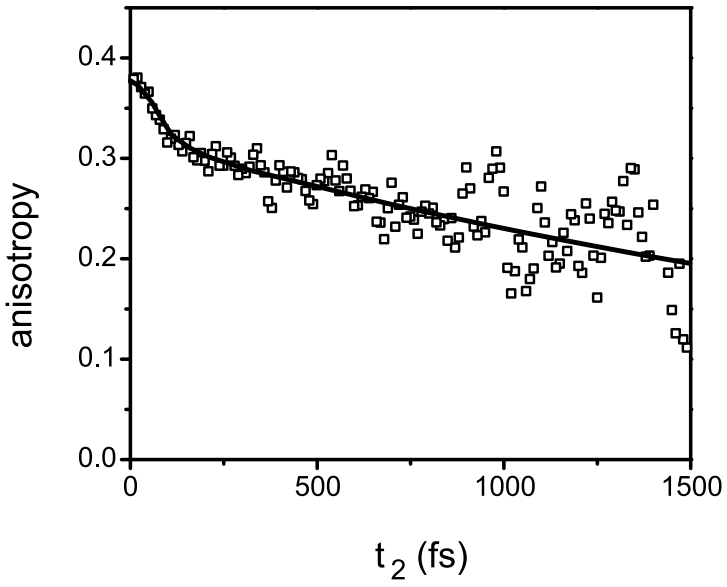

FIG. 8. Anisotropy of the O–H stretch vibration of HDO dissolved in D_2O as a function of delay measured with ultrashort (45 fs), broad-band (400 cm^{-1}) pump and probe pulses with a central frequency of 3400 cm^{-1} (courtesy of Andrei Tokmakoff). The anisotropy shows a bi-exponential decay with a fast component in the first 200 fs. Reproduced with permission from *J. Chem. Phys.* **2005**, *122*, 054506.

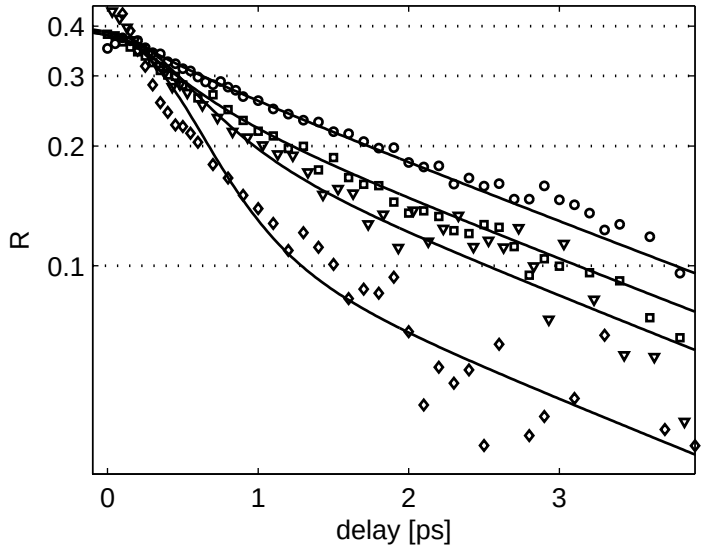

FIG. 9. Anisotropy of the O–D stretch vibration of HDO dissolved in H_2O as a function of delay for the same pump and probe frequency of 2500 cm^{-1} (circles), 2550 cm^{-1} (squares), 2600 cm^{-1} (triangles), and 2650 cm^{-1} (diamonds). The points denote the experimental data, the solid lines represent the results of calculations performed with the model described in Appendix B.

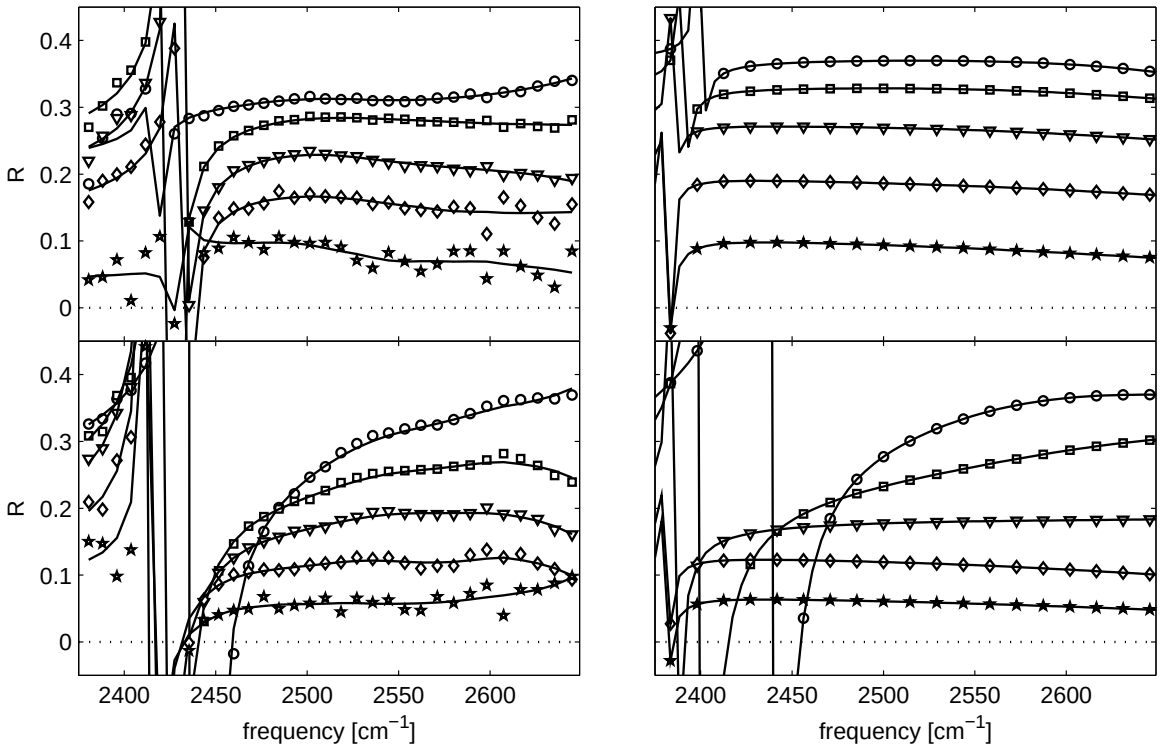

FIG. 10. Anisotropy as a function of frequency at delays of 0.2 ps (circles), 0.5 ps (squares), 1 ps (triangles), 2 ps (diamonds), and 4 ps (stars). Shown are results obtained with a pump frequency of 2500 cm^{-1} (upper panels), and 2600 cm^{-1} (lower panels). The left panels show the experimental results, the right panels present calculated results obtained with the model described in Appendix B.

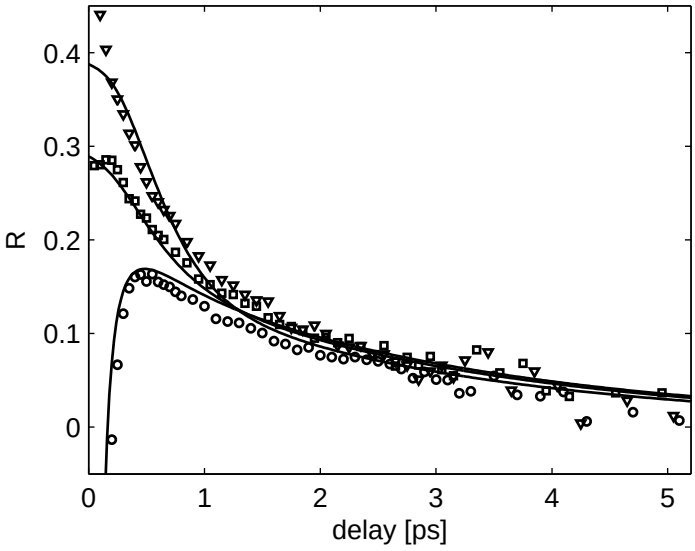

FIG. 11. Anisotropy of the O–D stretch vibration of HDO dissolved in H_2O as a function of delay measured for a pump frequency of 2650 cm^{-1} and probe frequencies of 2500 cm^{-1} (circles), 2550 cm^{-1} (squares), and 2600 cm^{-1} (triangles). The points denote the experimental data, the solid lines represent the results of calculations performed with the model described in Appendix B.